

Anode materials for lithium-ion batteries with nickel, copper and carbon

Danuta Olszewska^{1*} , Gabriel Borowski² 

¹ Faculty of Energy and Fuels, AGH University of Krakow, AGH University of Krakow, Al. A. Mickiewicza 30, 30-059 Krakow, Poland

² Faculty of Environmental Engineering and Energy, Lublin University of Technology, ul. Nadbystrzycka 40B, 20-618 Lublin, Poland

* Corresponding author's e-mail: dolszew@agh.edu.pl

ABSTRACT

Graphite, as a form of carbon, is used in many types of Li-ion batteries. The electrochemical properties of graphite are very good for these applications. However, increasing the volume of the cell during the discharge/charge process of the battery is not a desirable feature. This can lead to overheating or even explosion of the cell. Therefore, the materials that can replace graphite are sought. Such a material can be a composite consisting of $\text{Li}_4\text{Ti}_5\text{O}_{12}$ with a carbon material doped with copper and nickel ions. In this case, the addition of sucrose was used for better dispersion of these ions. In this way, the conductivity of the material can be improved. Anodes without carbon addition based on $\text{Li}_4\text{Ti}_5\text{O}_{12}$ (LTO) do not change their volume during discharge/charge cycles, but have low conductivity. A significant aspect of the use of sucrose in this composite is the lack of soot addition to the cell anode. Hence, the discussed composites significantly contribute to environmental protection and safety of selected Li-ion cells. In this work, three new anode materials with stoichiometric composition $\text{Li}_{3.8}\text{Cu}_x\text{Ni}_{0.2-x}\text{Ti}_5\text{O}_{12}$ calcined with 10% sucrose were synthesized. A positive effect of sucrose addition on the cell anode operating parameters was demonstrated. Among the materials tested the preferred composition of material composition is $\text{Li}_{3.8}\text{Cu}_{0.05}\text{Ni}_{0.15}\text{Ti}_5\text{O}_{12}\text{-C}$.

Keywords: Li-ion batteries, carbon, nano-composite; lithium intercalation, charge/discharge cycle, $\text{Li}_4\text{Ti}_5\text{O}_{12}$

INTRODUCTION

Lithium-ion batteries were widely used for a long time [1, 2]. The use of lithium-ion batteries today is common. The global market for these cells in 2012 was worth \$11.7 billion [3]. They have many advantages, but they also have certain disadvantages. For instance, when lithium is used as the anode [4], there are very frequent cases of overheating, or even ignition of the battery, which this contributes to the perception that this type of battery is hazardous.

It is difficult not to mention the ideal anode material for lithium batteries, which is metallic lithium, due to its numerous advantages. It is a material characterized by theoretical capacity of proximately $3825 \text{ mAh}\cdot\text{g}^{-1}$, constant and very low standard potential of -3.036 V relative to the

hydrogen electrode. However, the advantages of metallic lithium are not sufficient enough to make it willingly used on a large scale in commercial applications. The greatest disadvantage of using metallic lithium anodes is the instability of operation during cyclic charging/discharging of the cell. During intercalation/deintercalation, dendrite growth occurs on the surface on the metallic lithium anode. It is stronger the higher the current density the cell is charged with. This phenomenon, apart from determining the effective operation of the cell, is very dangerous, because it leads to an internal short circuit of the cell.

Therefore, graphite is an alternative to lithium anode. Due to its characteristics, the use of graphite as anode material turned out to be a better solution than in the case of metallic lithium. Graphite is a cheap and easily available material

in the natural environment, and has high chemical as well as thermal stability. It is also characterized by high electrical conductivity and a high theoretical capacity of $372 \text{ mAh}\cdot\text{g}^{-1}$ for the intercalation of graphite with lithium in the LiC_6 composition, hence this material has found wide commercial application.

Graphite may be also used as the cathode material in new dual-ion batteries DIB due to its layered structure enabling reversible anion storage, environmental friendliness and low cost [5]. Dual-ion batteries are a novel battery technology that can meet various key requirements such as long life, low cost and ease of recycling. Potassium-based dual ion batteries are new potential materials for replacing traditional Li-ion batteries [6]. During the charging process, cations like Li^+ , K^+ , are inserted or deposited on the e.g. graphite or metal Li/K anode, while anions are intercalated in the graphite cathode. The cell chemistry and charging/discharging mechanism of DIBs are different from conventional LiBs. In DIB, the cathode supplying the Li^+ cation is replaced by an anion storage material, while the salt in the electrolyte is considered as the active material. The intercalation of anions on the cathode enables high cell voltages of up 5.2 V, i.e. beneficial for achieving high energy density.

The anode of Li-ion batteries is one of the key elements of the batteries and has an impact on the above-mentioned properties of cells [4, 7]. Despite many advantages, including low price, easy availability, non-toxicity and good electrical conductivity, graphite is not a material without drawbacks [8, 9]. During the intercalation/deintercalation process, lithium changes its volume by approximately 10%, which may lead to graphite grain cracking and, consequently, to a reduction in the specific capacity of the cell and degradation of the anode. Graphite is a highly reactive material with limited volumetric capacity and low level of safety. Moreover, in lithium cells there is a negative phenomenon of dendrite growth. That is because the intercalation potential with Li^+ ions is approximately 100 mV, and highly reactive metallic lithium, when charged with high density currents, is deposited on the electrode surface, forming dendrites. This may pose a risk of short circuiting the cell and, consequently, lead to fires.

One of the most difficult tasks standing in the way of commercialization of Li-ion cell technology—application, among others, in electric cars, is the development of appropriate electrode

materials and electrolytes. From a technological point of view, it is crucial to select the materials with high energy and power density, with a sufficiently high electromotive force of the cell, cheap to produce and safe for the natural environment. The most common requirements for cathode and anode materials are high gravimetric and volumetric amount of stored energy, high redox potential towards lithium ($>3 \text{ V}$) for the cathode material and low redox potential towards lithium ($<0.5 \text{ V}$) for the anode material, appropriately high ion-electron conductivity of the electrode material at the cell operating temperature, high thermal and chemical stability, high reversibility of the intercalation process ensuring long cell life (over 500 cycles), relative easy and cheap preparation, non-toxic to the natural environment. In practice, no ideal electrode materials for Li-ion cell have been found so far. That is why the compromise between the minimum requirements for safe use and the operating parameters of such a cell is so important.

Of course, metallic lithium and graphite are not only known anode materials. Currently, the most commonly used anode material is other carbon materials. For example Breczko et al. [10] compared the capacitance properties of selected fullerene-containing electroactive materials for batteries and electrochemical capacitors. Materials based on intermetallic alloys are also described in the literature [11]. This group consist of alloys of lithium with other elements, for example tin, silicon or aluminum. In the case of three-component alloys, during the reaction with lithium, one of the alloy components forms an alloy with lithium, while the other constitutes a protective matrix. Among titanium-based materials, titanium oxides is one of the more attractive anode materials [12]. The crystallographic structure TiO_2 contains octahedra (TiO_6), arranged in the spatial lattice in the different ways, depending on the polymorphic variety. Titanium dioxide occurs naturally in the three varieties: anatase, rutile and brookite, with both anatase and rutile belonging to the tetragonal crystallographic system. The most stability of TiO_2 phase from a thermodynamic point of view is rutile. This phase transition from anatase to rutile is irreversible and occurs at a temperature of approximately 600°C . Maximum theoretical capacity is $335 \text{ mAh}\cdot\text{g}^{-1}$ and corresponds to the reduction of titanium ions from the oxidation state of +4 to +3. This corresponds to a working potential in the range of

1.4–1.8 V relative to $\text{Li}|\text{Li}^+$, with a plateau at a voltage of approximately 1.7 V. The specific capacitance is determined by the degree of intercalation of the compound. The advantages of TiO_2 undoubtedly include high chemical stability, good stability during the intercalation process, safety and low cost. However, the disadvantages are low specific capacity for grains of micrometer size. Orthorhombic Nb_2O_5 ($\text{T-Nb}_2\text{O}_5$) is another intercalation-type anode material. The multielectron redox reaction enables a high theoretical capacity ($200 \text{ mA} \cdot \text{h} \cdot \text{g}^{-1}$) [13]. Examples of anode materials are listed.

Thus, graphite, seems to be the best option. Unfortunately, graphite material, in spite of its advantages has also some drawbacks; in particular, they are associated with mechanical properties and strength. For this reason, other forms of carbon are increasingly used in lithium-ion batteries [7]. Instead of carbon in the form of graphite, it was proposed to use carbon from sucrose. Replacing graphite with another form of carbon material has been reported in literature. These studies are carried out on a large scale. As it is known, the carbon has various forms [15, 16]. One of these is carbon black [14] that is added to the electrode compounds to improve the electrochemical properties of the battery [15, 17] or acetylene black [18, 19], a type of carbon black, obtained from thermal decomposition of acetylene [20]. The carbonaceous material in the form of graphite or carbon black is typically added to the cathode compound materials in an amount of 25 wt.% (15% graphite and 10% carbon black) [21]. Depending on the application, the addition of carbonaceous component to the electrode material is from 5 to 20% by weight. On an industrial scale, carbon black was produced after developing the method for obtaining carbon black conduit (1892), followed by a furnace method (1947), most commonly used today. Preparation of carbon black is based on the combustion of various kinds of hydrocarbon-based materials (i.e., oil or natural gas) with limited access to air. Furnace black process is now the most popular method in which kerosene oil or carbon is blown into high-temperature gases to cause their partial combustion. Other techniques for obtaining carbon black is a channel method (in which the soot is deposited on the steel profile), acetylene (explosive decomposition of acetylene) and lamp (the oldest, which consists of collecting soot from the smoke evolved during the combustion of oil

or wood). As it can be seen, the addition of carbon to lithium batteries caused the increase of production of carbon black. The paper proposed an alternative approach, having regard to the particular environment and the elimination process by use of hydrocarbons. Instead of the addition of carbon black added to the material of the anode or cathode in the process of constructing the battery, a synthesis of the anode material with the addition of sucrose was proposed, which eliminated the need to introduce additional carbon to lithium batteries. An innovative solution that can greatly affect the environmental aspect of the production of batteries. Unlike the carbon black, sucrose is a generally available, inexpensive compound. After application of appropriate preparation steps of anode material containing carbon present in sucrose, not only the electrochemical properties of the electrode material, but also their structural properties are improved.

The authors proposed to add sucrose to montmorillonite materials used as catalysts for the removal of nitrogen oxides by selective reduction of nitrogen oxides from flue gases from coal combustion [22, 23] and Olszewska [24] described sucrose as an additive to reduce the emission of sulfur oxides in the co-incineration of coal [25, 26].

Graphite has very good electrochemical parameters, but it is not a suitable material in mechanical terms. Spinel has worse properties than graphite, but are better mechanically. It is possible to make such combinations of carbon material and spinel that will optimally utilize the best properties of both materials and compensate the worse ones. The author proposed just such a solution of carbon material with anode material spinel $\text{Li}_4\text{Ti}_5\text{O}_{12}$ (LTO) [27]. Lithium titanium oxides with a spinel structure constitute an interesting substitute for carbon materials for anodes of lithium-ion cell. They show high thermodynamic stability with voltage plateau at approximately 1.55 V, which excludes the reduction of electrolyte on the electrode surface and increases the safety of the battery in use. Moreover, they are characterized by exceptionally high reversibility of the introduction and removal of Li^+ ions into and out of the structure, in the voltage range 1.0–2.5 V, good service life, and good theoretical capacity of approximately $175 \text{ mAh} \cdot \text{g}^{-1}$.

Their advantage is that they do not change their volume when using the battery, which makes them attractive for security reasons. However, they have very low electrical conductivity [28].

In addition, in this case carbon black is used in order to increase the conductivity of LTO. Sucrose addition to oxide materials is applied in various fields of technology.

The paper presents the results of a research on the system, which was abandoned with soot, modifying the anode material by the use of sucrose in addition to the LTO material in order to increase its conductivity without reducing safety. It was based on reports of successful use of glucose or sucrose as a $\text{Li}_4\text{Ti}_5\text{O}_{12}$ additive [28, 29]. Equally, the LTO spinel doped with copper and nickel to increase its conductivity, electric capacity and stability of the structure [18]. Energy storage for portable electronic devices and electric vehicles consists in accumulating energy in batteries. Currently, this role is largely played by Li-ion cells [3, 7]. These energy storage devices use high energy and power density as well as extended cell life cycles [14, 15]. Battery efficiency is their important feature. Graphite or $\text{Li}_4\text{Ti}_5\text{O}_{12}$ (LTO) are commercially used as anodes in cells. The former material is characterized by appropriate electrochemical properties. Its common use is excluded by one parameter: the difference in cell volume after intercalation/deintercalation cycles. This creates a measurable explosion hazard during use. Therefore, LTO is an optimal alternative to carbon-based anodes [17, 18]. In $\text{Li}_4\text{Ti}_5\text{O}_{12}$ cells, the lattice parameter practically does not change during lithium intercalation and deintercalation [21]. LTO has a high working potential (~ 1.55 V compared to Li/Li^+) [19, 20]. This leads to a significant reduction in energy density. However, the working potential occurs in the thermodynamic stability window of the electrolyte solutions, so it is not necessary to form an SEI layer for the proper functioning of the electrode. The $\text{Li}_4\text{Ti}_5\text{O}_{12}$

electrode is characterized by a long cycle life, is resistant to overcharging and can be used in a suitable, wide temperature range [20]. After introducing 3 moles of Li^+ into the $\text{Li}_4\text{Ti}_5\text{O}_{12}$ structure, the theoretical capacity of LTO is $175 \text{ mAh} \cdot \text{g}^{-1}$. In the stable structure $[\text{Li}_3]^{8a}[\text{LiTi}_5]^{16d}[\text{O}_{12}]^{32e}$, all tetrahedral positions (8a) and 1/6 of the 16d position are occupied by lithium atoms, and the remaining 5/6 of the 16d position are occupied by titanium atoms. Oxygen atoms occupy the 32e positions, and the octahedral (16c) positions are empty [22, 23]. After introducing lithium ions, the $\text{Li}_4\text{Ti}_5\text{O}_{12}$ structure changes to the rock salt structure $\text{Li}_7\text{Ti}_5\text{O}_{12}$, the skeleton of which is described as $[\text{Li}_6]^{16c}[\text{LiTi}_5]^{16d}\text{O}_{12}$ [22]. The disadvantage of LTO is its low electronic conductivity ($10^{-13} \text{ S} \cdot \text{cm}^{-1}$) [24]. Therefore, research is being conducted on the optimization and improvement of electronic and ionic conductivity of LTO. The modification may consist in obtaining a material with a relatively large surface area and small grain size [25, 26], adding various metal cations [27, 28] or preparing composites with carbon material [29].

EXPERIMENTAL

Synthesis

Synthesized samples $\text{Li}_{3.8}\text{Cu}_x\text{Ni}_{0.2-x}\text{Ti}_5\text{O}_{12}\text{-C}$ (where x is equal to 0.15, 0.10, 0.05) were obtained by solid state synthesis using Li_2CO_3 , TiO_2 , CuO , NiO and sucrose (Aldrich 99.99%). Stoichiometric amounts of the precursors were mixed in a high-energy mill for 20 min and dried in the air at 70°C for 2 hours. The powders were pressed to give tablets, which were then calcined at 800°C under argon for 4 hours. Figure 1 presents the scheme of preparation.

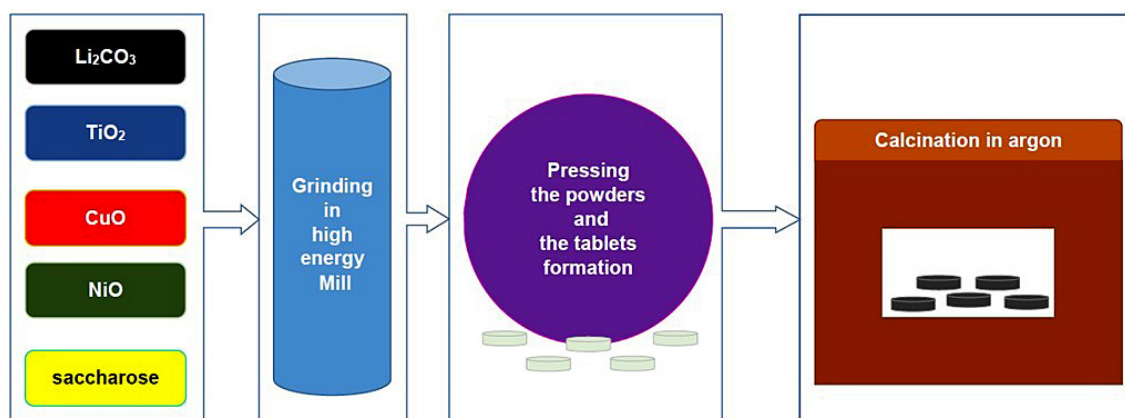


Figure 1. The scheme of samples preparation

Research methods

Morphology and microstructure of prepared samples were observed by scanning electron microscopy (SEM) at different magnifications. In addition, the selected point analyses were performed by EDS. Morphology and structure of samples were analyzed by NanoSEM 200 FEI scanning electron microscope equipped with low vacuum detector (LVD). The particle size was obtained using SEM analysis.

The resulting pelletized materials were subjected to impedance spectroscopy to determine the conductivity of the materials. The conductivity of sample pellets was measured using impedance spectroscopy with frequency response analyzers, Solatron 1260 from room temperature (27°C) in order to determinate the conductivity.

Other electrochemical measurements were performed using appropriately prepared cell. Each electrode was prepared by mixing the active material ($\text{Li}_{3.8}\text{Cu}_x\text{Ni}_{0.2-x}\text{Ti}_5\text{O}_{12}\text{-C}$) and the binder poly (vinylidene fluoride) (PVDF) powder in a weight ratio of 95:5 (as appropriate) or 80:10:10 (respectively, active material with sucrose $\text{Li}_{3.8}\text{Cu}_x\text{Ni}_{0.2-x}\text{Ti}_5\text{O}_{12}\text{-C}$:PVDF:carbon black) in a slurry solution of N-methyl-2-pyrrolidone. Those suspensions were spread on aluminum foil and dried at 80°C for 2 hours under reduced pressure. Aluminum foil bearing a mixture of the active material and the PVDF was cut in the form of discs with a diameter of 8 mm. The electrode served as a working electrode. Lithium metal was used as a counter electrode. A porous polypropylene film separator impregnated with the electrolyte solution was placed between the electrodes.

The electrolyte applied was $1 \text{ mol}\cdot\text{dm}^{-3} \text{ LiPF}_6$ in a mixture of ethylene carbonate and diethyl carbonate in a volume ratio of 1:1. Cells were assembled in a glove box. Cell cases CR2023 were used in order to close the cell. The scheme of cells is presented in Figure 2.

Cyclic voltammetry studies were carried out on the cells obtained by applying to the cell a linearly changing voltage over time at a rate of $0.1 \text{ mV}\cdot\text{s}^{-1}$ (in the range of 2.0 to 1.3 V and from 1.3 to 2.0 V) and measuring current flowing through the cell. For each of the materials three cycles of measurement of cyclic voltammetry were performed. In order to determine the appropriate capacity, the cells were periodically charged and discharged in the voltage range of 1.3 to 2.0 V for various values of the charge/discharge current (0.1C and 5C). All measurements were done at room temperature. The C rate was calculated based on the weight of the electrode and theoretical capacity of LTO. Cells were tested at a computer-controlled galvanostat (KEST 32k multichannel) and on the electrochemical test instrument (ATLAS). All the electrochemical tests were carried out at room temperature.

RESULTS AND DISCUSSION

Structure determination

Figures 3–5 include a series of photographs of $\text{Li}_{3.8}\text{Cu}_{0.15}\text{Ni}_{0.05}\text{Ti}_5\text{O}_{12}\text{-C}$ samples at following magnifications: 10000, 30000, and 50000 times. The analysis of the composition of the material at a selected point was performed by EDS.

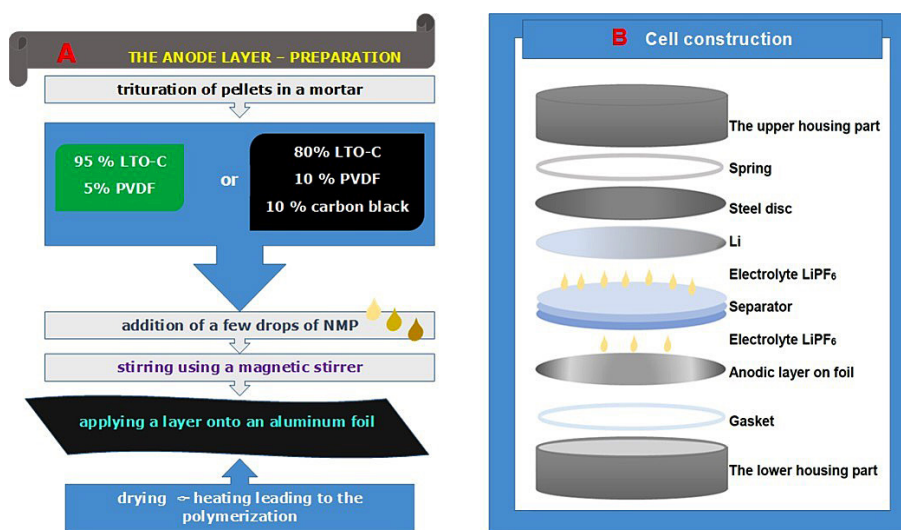


Figure 2. The scheme of cells: A – the anode layer preparation; B – cell construction

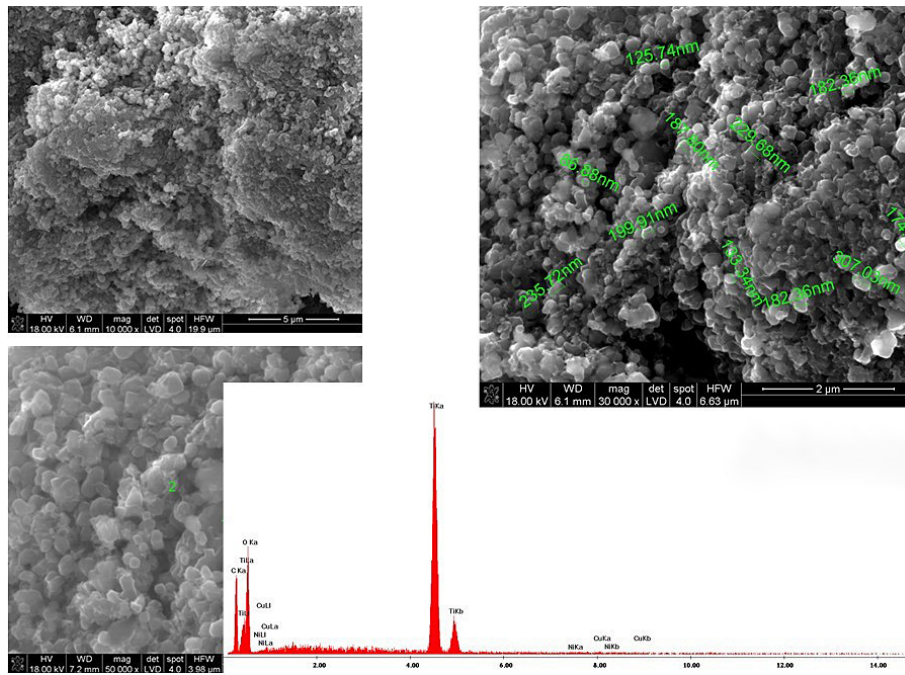


Figure 3. Images of electron scanning microscope (SEM) of powder $\text{Li}_{3.8}\text{Cu}_{0.15}\text{Ni}_{0.05}\text{Ti}_5\text{O}_{12}\text{-C}$. Magnification: 10000 \times ; 30000 \times (with marked dimensions of grain size) and 50000 \times , point 2 measured by the EDS method)

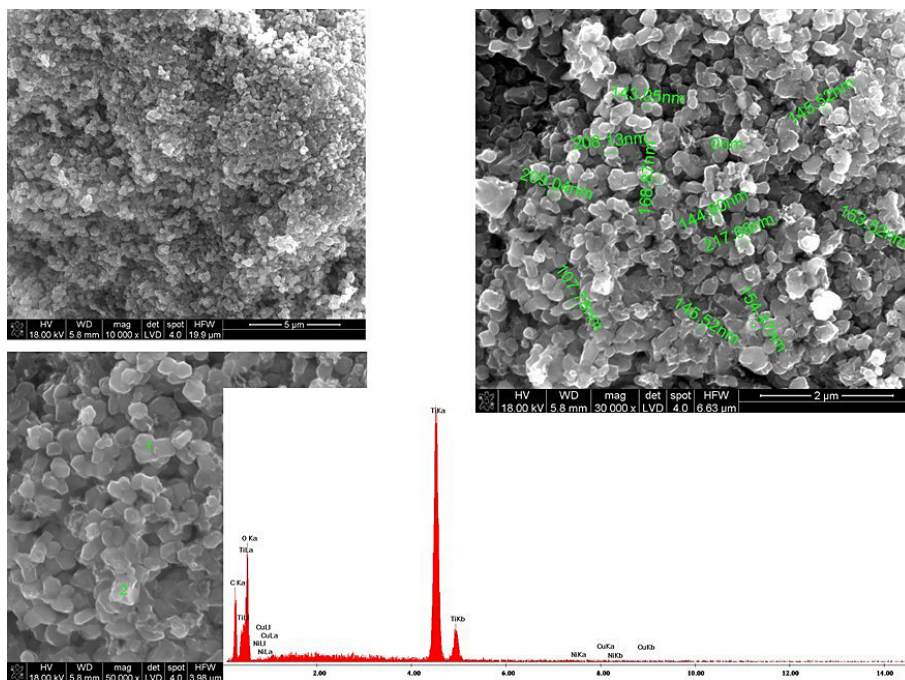


Figure 4. Images of electron scanning microscope (SEM) of powder $\text{Li}_{3.8}\text{Cu}_{0.1}\text{Ni}_{0.1}\text{Ti}_5\text{O}_{12}\text{-C}$. Magnification: 10000 \times ; 30000 \times (with marked dimensions of grain size) and 50000 \times , point 2 measured by the EDS method)

The result of SEM confirmed that test samples contain no metallic nickel or copper. Figure 6 shows the grain sizes for the tested samples [nm]. SEM images show visible agglomerates consisting of aggregates with a size of 86–300 nm. From the measurements, it was observed

that the average grain size of the samples containing the minimum and maximum amount of Cu was 185 nm. A material with the same amount of copper and nickel has a smaller average grain size of 165 nm.

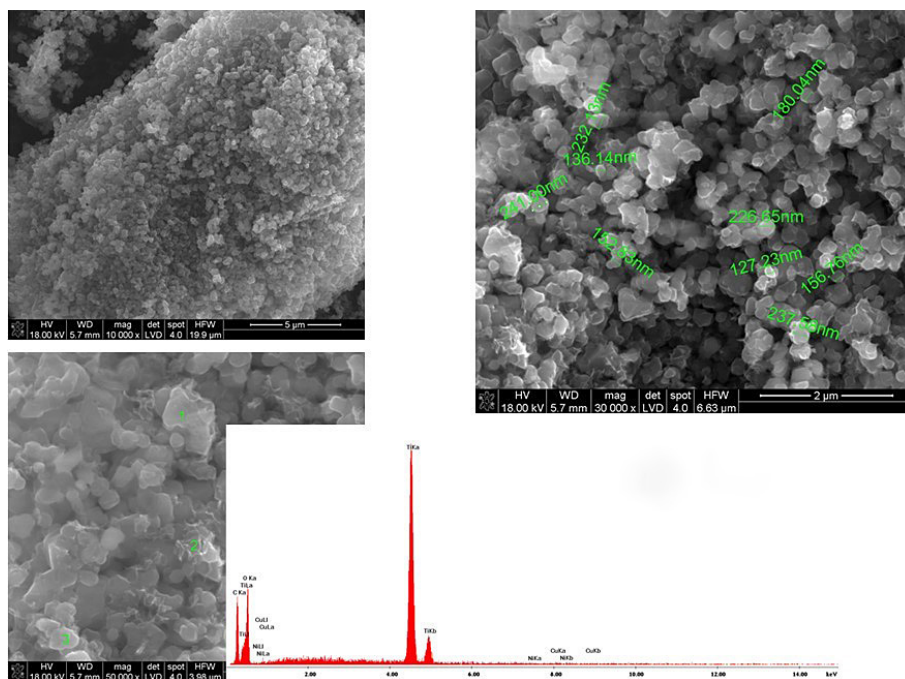


Figure 5. Images of electron scanning microscope (SEM) of powder $\text{Li}_{3.8}\text{Cu}_{0.05}\text{Ni}_{0.15}\text{Ti}_5\text{O}_{12}\text{-C}$. Magnification: 10000 \times ; 30000 \times (with marked dimensions of grain size) and 50000 \times , point 2 measured by the EDS method)

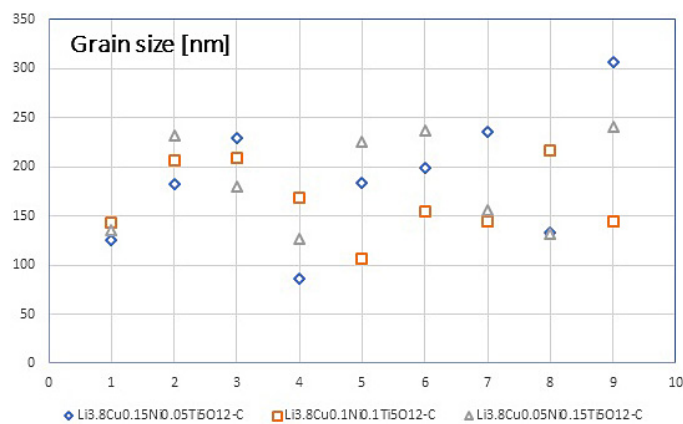


Figure 6. Grain sizes of obtained samples

Conductivity

The following section presents the results of measurements of the electrical conductivity of sintered materials using the impedance spectroscopy. The topic of testing the conductivity by impedance spectroscopy of lithium-titanium spinel in the form of polycrystalline sinters is not widely described in the literature. Moreover, there are not no reports describing the conductivity of materials with the addition of Cu^{2+} and Ni^{2+} or two-phase materials. The first reports on specific conductivity of $\text{Li}_4\text{Ti}_5\text{O}_{12}$ appeared in the publication of Ferga et al. [30] from 1994, but the method of determining the conductivity and its value are currently controversial. It was indicated

that the conductivity of LTO at room temperature is approximately $10^{-13} \text{ S}\cdot\text{cm}^{-1}$. In spite of the merits mentioned above, low conductivity ($10^{-13} \text{ S}\cdot\text{cm}^{-1}$) hinders the further enhancement of LIB performance [31]. Srout et al. [32] studied EIS of metallic lithium anodes. The authors compared EIS spectra for thin and thick Li-metal anodes. Measurements of the electrical conductivity of pure spinel pellets and those modified with copper and nickel ions were carried out by impedance spectroscopy using a Solatron 1260 frequency response analyzer. Measurements were carried out in the frequency of 0.1Hz – 1 MHz, with a voltage excitation amplitude of 100 mV. In order to ensure good contact between the sample and the electrical leads, electrodes in the form of Au paste

(ESL ElectroScience 8844G) were applied to the polished surfaces at 800°C for 15 minutes. The error in the measurement of electrical conductivity may include uncertainty in the measurement of two geometric dimensions of the sample – the thickness and diameter of the sinter disc, uncertainty of determining the resistance based on the measured impedance spectrum. The maximum error of each of these factors should not exceed 5%; therefore, the maximum error of the conductivity measurement was estimate at 15%.

Conductivity of the samples obtained was measured using impedance spectroscopy. The test results are shown in Table 1. Due to the complex composition of samples, the total conductivity was calculated, related to the pellet dimensions, for the given materials.

The material $\text{Li}_{3.8}\text{Cu}_{0.1}\text{Ni}_{0.1}\text{Ti}_5\text{O}_{12}\text{-C}$ ($7.32 \text{ mS}\cdot\text{cm}^{-1}$) has the highest conductivity. Material $\text{Li}_{3.8}\text{Cu}_{0.05}\text{Ni}_{0.15}\text{Ti}_5\text{O}_{12}\text{-C}$ has slightly lower conductivity ($6.65 \text{ mS}\cdot\text{cm}^{-1}$). Conductivity of material $\text{Li}_{3.8}\text{Cu}_{0.15}\text{Ni}_{0.05}\text{Ti}_5\text{O}_{12}\text{-C}$ differs significantly from the values of conductivity of the other samples, and is only $2.27 \text{ mS}\cdot\text{cm}^{-1}$. The mechanism of influence of copper in the LTO structure on the material conductivity is complex. Copper, due to its high electronic conductivity, is a very good conductor and when placed in a structure, it improves conductivity [33, 34]. However, the correlation of the specific conductivity of samples with the copper content is not a linear relationship. Maxima are visible, with different copper content depending on the tested materials. Lin et al. [33] and Bai et al. [35] also noticed that the resistance of copper samples was lower than that of pure LTO samples, but conductivity did not change linearly with the increase in/of the amount of substituted ion, it was non-monotonic after the optimum, the conductivity value decreased. This is probably due to the superposition of two effects, which, when combined, cause the conductivity to increase non-linearly until it reaches a maximum and then decreases. Sometimes a second growth is also observed. A positive effect is the improvement of transport properties for doped samples

due to partial change in the oxidation state of titanium from +4 to +3 oxidation state and an increase in the number of charge carriers due to doping with d-electron metals. The second effect is caused by the difference in ionic radii between Li^+ , Cu^{2+} , Ti^{4+} and Ti^{3+} ions. Changing these radii causes a slight increase in the lattice parameter of the unit cell, but this increase is so small that the diffusion path becomes narrowed, which worsen the diffusion of the Li^+ ions.

To sum up, the introduction of d-electron metal ions into the structure of lithium-titanium spinel improves the conductivity of the materials. Substituted ions with electrons 3d orbitals may facilitate the hopping conduction mechanism, but on the other hand, they may hinder the diffusion mechanism through diffusion channels. Very detailed EIS studies were carried out by Scarpioni et al. [36] for batteries with liquid electrolytes.

Cyclic voltammetry

Cell measurements using cyclic voltammetry were carried out in the voltage range of 1.3-2.0 V. The selected interval is within the electrochemical window of the electrolyte used. Cyclic voltammetry studies were carried out on cells containing $\text{Li}_{3.8}\text{Cu}_x\text{Ni}_{0.2-x}\text{Ti}_5\text{O}_{12}\text{-C}$ as an active material of working electrode. The results in Figure 7 present differential capacity curves calculated for the studied $\text{Li}|\text{Li}^+|\text{Li}_{3.8}\text{Cu}_{0.1}\text{Ni}_{0.1}\text{Ti}_5\text{O}_{12}\text{-C}$ cells – dQ/dE [$\text{mAh}\cdot\text{V}^{-1}\cdot\text{g}^{-1}$] function of the Li/Li^+ potential for second cycles was shown. Differential capacity curves of electrodes containing materials $\text{Li}_{3.8}\text{Cu}_{0.15}\text{Ni}_{0.05}\text{Ti}_5\text{O}_{12}\text{-C}$ and $\text{Li}_{3.8}\text{Cu}_{0.05}\text{Ni}_{0.15}\text{Ti}_5\text{O}_{12}\text{-C}$ are very correct and repeatable.

These values are characteristic for the electrodes containing LTO [37]. Differential capacity curves for $\text{Li}_{3.8}\text{Cu}_{0.1}\text{Ni}_{0.1}\text{Ti}_5\text{O}_{12}\text{-C}$ electrode (especially for the first measurement cycle) are not correct. In Figures 7 a, b and c it can be seen that the value of the anode potential increases with scanning speed (from 1.65 to 1.83 V) and the value of the cathode potential decreases (from 1.45 to 1.38 V). In accordance with literature, LTO also has a very flat voltage plateau at around 1.55V (vs. $\text{Li}|\text{Li}^+$) [38]. Cathode peaks occur for both samples at the average value of the potential approx. 1.45 V relative to a lithium electrode, while the anodic peak potential occur at the average value of the potential approx. 1.7 V relative to a lithium electrode. However, the anode and cathode peaks are not symmetrical to themselves and they are

Table 1. Conductivity of obtained samples

Sample	Conductivity [$\text{mS}\cdot\text{cm}^{-1}$]
$\text{Li}_{3.8}\text{Cu}_{0.15}\text{Ni}_{0.05}\text{Ti}_5\text{O}_{12}\text{-C}$	2.27039
$\text{Li}_{3.8}\text{Cu}_{0.1}\text{Ni}_{0.1}\text{Ti}_5\text{O}_{12}\text{-C}$	7.31926
$\text{Li}_{3.8}\text{Cu}_{0.05}\text{Ni}_{0.15}\text{Ti}_5\text{O}_{12}\text{-C}$	6.64977
$\text{Li}_4\text{Ti}_5\text{O}_{12}$	10^{-10}

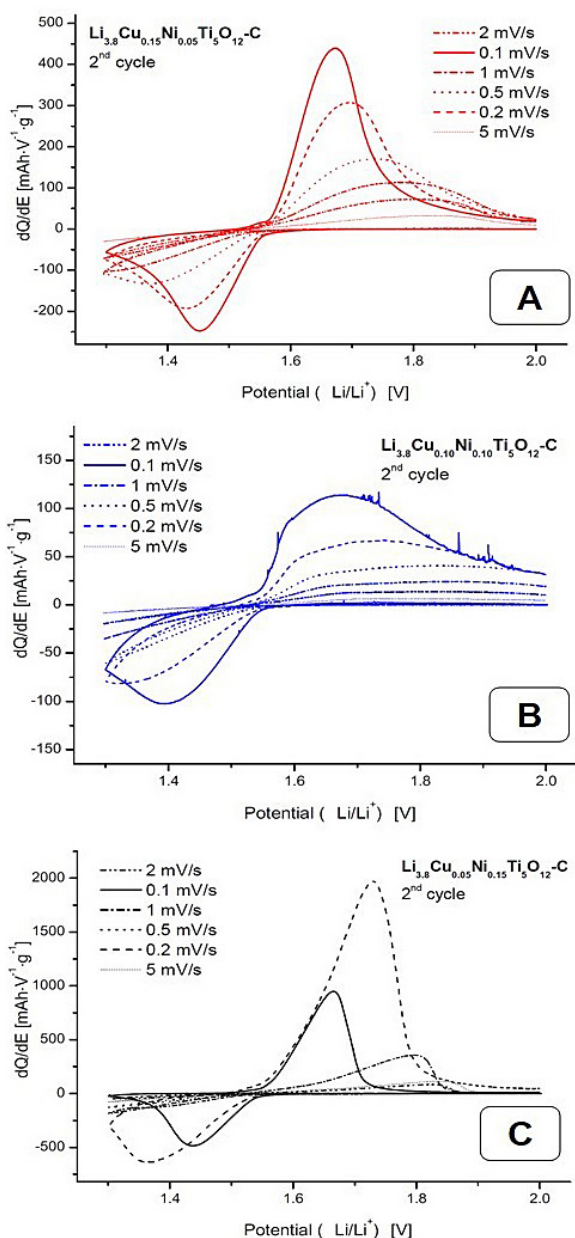


Figure 7. Plots of cyclic voltammetry as a function dQ/dE [mAh·V⁻¹·g⁻¹] of (Li/Li⁺) [V] potential values at different scan rate [mV·s⁻¹] for the second charge/discharge cycle of samples:
 a) $\text{Li}_{3.8}\text{Cu}_{0.15}\text{Ni}_{0.05}\text{Ti}_5\text{O}_{12}\text{-C}$, b) $\text{Li}_{3.8}\text{Cu}_{0.1}\text{Ni}_{0.1}\text{Ti}_5\text{O}_{12}\text{-C}$,
 c) $\text{Li}_{3.8}\text{Cu}_{0.05}\text{Ni}_{0.15}\text{Ti}_5\text{O}_{12}\text{-C}$

not spread out symmetrically in relation to each other either. Presumably, the reason for this can be a change of the mechanism of electrode processes or the existence of different phases (components) in the electrodes.

Charge/discharge test

Electrochemical characteristics of $\text{Li}|\text{Li}^+|\text{Li}_{3.8}\text{Cu}_x\text{Ni}_{0.2-x}\text{Ti}_5\text{O}_{12}\text{-C}$ cells with different

composition of the anode: a – 95% LTO-C:5% PVDV and (for comparison) b – 80% LTO-C:10% PVDV:10% carbon black are shown in Figure 8.

Charge/discharge curves are very similar for all tested materials. They differ in the values that are aggregated for comparison in a bar chart. The addition of sucrose during the preparation of anode materials replaces the addition of carbon black in further stages of battery preparation. The specific capacities of the $\text{Li}_{3.8}\text{Cu}_x\text{Ni}_{0.2-x}\text{Ti}_5\text{O}_{12}\text{-C}$ electrodes were measured.

Figure 9 presents the comparison of third discharge curves for cells $\text{Li}|\text{Li}^+|\text{Li}_4\text{Cu}_{0.1}\text{Ni}_{0.1}\text{Ti}_5\text{O}_{12}\text{-C}$ without (a) and with 10% wt. carbon black (b). By far, the lowest values were recorded for the capacity of the relevant electrode $\text{Li}_{3.8}\text{Cu}_{0.15}\text{Ni}_{0.05}\text{Ti}_5\text{O}_{12}\text{-C}$. In addition, this capacity fairly quickly decreases within the following charge/discharge cycles. The specific capacity of the electrode $\text{Li}_{3.8}\text{Cu}_{0.1}\text{Ni}_{0.1}\text{Ti}_5\text{O}_{12}\text{-C}$ is much more stable. The electrode maintains a capacity exceeding 100 mAh·g⁻¹, even at a current value of 1C. Unfortunately, no stability tests were performed. As it is known, such tests require repetitions of at least 100 cycles. It is known from previous research on LTO that these are materials with high stability [17]. In the performed tests, charging/discharging cycles were repeated 10 times.

The highest values were recorded for the capacity of the relevant electrode $\text{Li}_{3.8}\text{Cu}_{0.05}\text{Ni}_{0.15}\text{Ti}_5\text{O}_{12}\text{-C}$. The maximum value of capacity of this electrode is approx. 160 mAh·g⁻¹ at current equal to 0.1C. At a current value equal to 1C the capacity of this electrode is practically constant in subsequent cycles of charge/discharge and it is higher than 120 mAh·g⁻¹. For the current equal to 2C discharge capacity of the electrode drops below 100 mAh·g⁻¹. The dependence of capacity on the potential of the working electrode relative to lithium for the third discharge cycle was also checked. For lower current values (0.5C and 0.2C for $\text{Li}_{3.8}\text{Cu}_{0.15}\text{Ni}_{0.05}\text{Ti}_5\text{O}_{12}\text{-C}$ and of 0.1C to 1C $\text{Li}_{3.8}\text{Cu}_{0.1}\text{Ni}_{0.1}\text{Ti}_5\text{O}_{12}\text{-C}$ and $\text{Li}_{3.8}\text{Cu}_{0.05}\text{Ni}_{0.15}\text{Ti}_5\text{O}_{12}\text{-C}$), one can see a broad plateau covering almost the entire capacity range of the working electrode potentials in the range between 1.55 and 1.6 V relative to the lithium electrode.

The potential of that plateau is lower for higher currents. The course of the relationship between specific capacity and the potential of the electrode is characteristic for LTO [25]. Similar research was carried out by Yang et al.

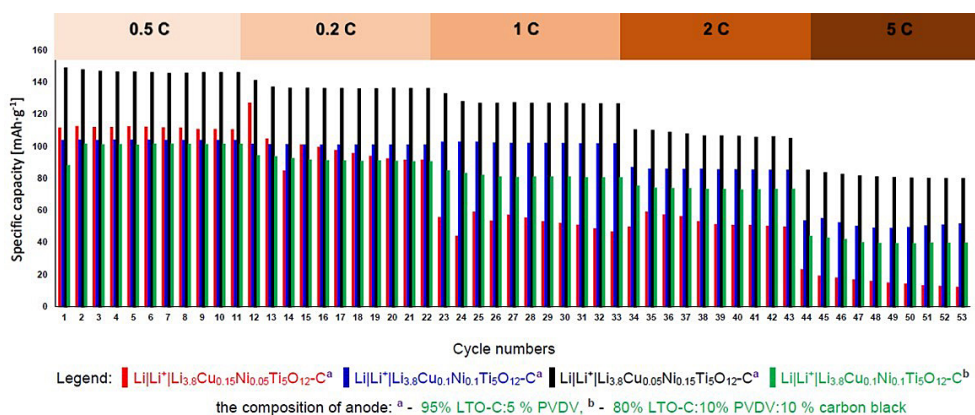


Figure 8. The comparison of electrochemical properties obtained samples. The composition of anode: a) – 95% LTO-C:5% PVDV, b) – 80% LTO-C:10% PVDV:10% carbon black. As the LTO-C: $\text{Li}|\text{Li}^+|\text{Li}_{3.8}\text{Cu}_{0.15}\text{Ni}_{0.05}\text{Ti}_5\text{O}_{12}\text{-C}$, $\text{Li}|\text{Li}^+|\text{Li}_{3.8}\text{Cu}_{0.1}\text{Ni}_{0.1}\text{Ti}_5\text{O}_{12}\text{-C}$, $\text{Li}|\text{Li}^+|\text{Li}_{3.8}\text{Cu}_{0.05}\text{Ni}_{0.15}\text{Ti}_5\text{O}_{12}\text{-C}$, $\text{Li}|\text{Li}^+|\text{Li}_{3.8}\text{Cu}_{0.1}\text{Ni}_{0.1}\text{Ti}_5\text{O}_{12}\text{-C}$

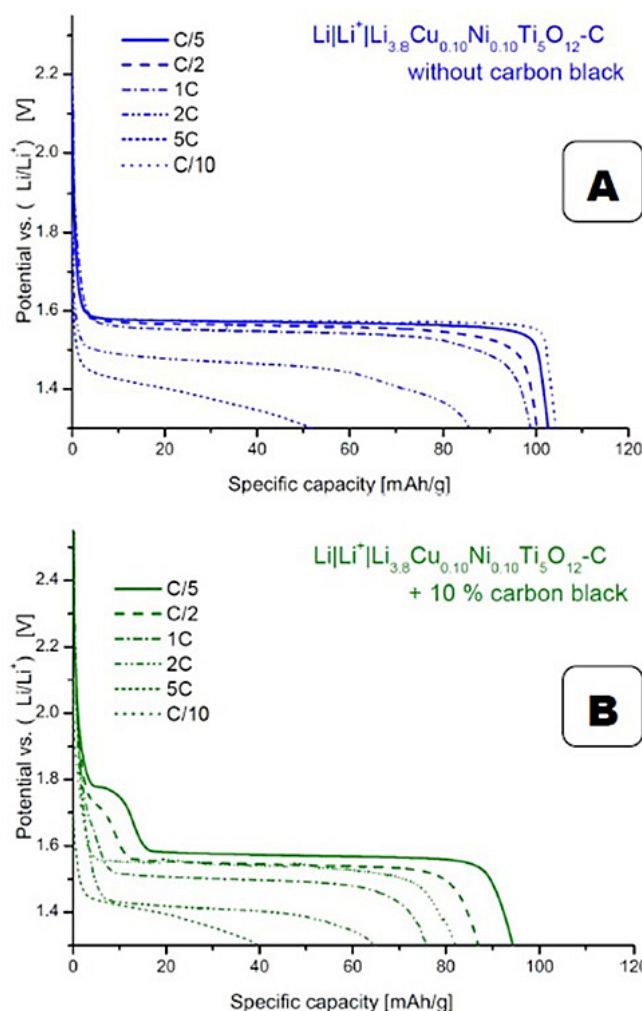


Figure 9. Comparison of 3rd discharge curves for cells $\text{Li}|\text{Li}^+|\text{Li}_4\text{Cu}_{0.1}\text{Ni}_{0.1}\text{Ti}_5\text{O}_{12}\text{-C}$ without (a) and with 10% wt. carbon black (b)

[26], but citric acid was used as a precursor of coal. On the basis of the study, the electrodes prepared without carbon black worked much better than that of LTO.

Cunha et al. [41] reported the electrochemical performance of epitaxial $\text{Li}_4\text{Ti}_5\text{O}_{12}$ films with different orientations. (100)-oriented $\text{Li}_4\text{Ti}_5\text{O}_{12}$ films shows the highest capacities ($313 \text{ mA}\cdot\text{h}\cdot\text{g}^{-1}$),

excellent rate performance, and good cyclability with improved cycle life and doubling of reversible capacities compared to the polycrystalline $\text{Li}_4\text{Ti}_5\text{O}_{12}$ in different studies.

CONCLUSIONS

All materials obtained during the study consist of LTO; the main phase is $\text{Li}_4\text{Ti}_5\text{O}_{12}$, the other phases are TiO_2 and Li_2TiO_3 . The compositions of the different phases for three materials obtained are similar. The composition of the sample $\text{Li}_{3.8}\text{Cu}_{0.05}\text{Ni}_{0.15}\text{Ti}_5\text{O}_{12}\text{-C}$ is the most distinguished. It has the largest share of LTO phase and Li_2TiO_3 and the lowest share of mass phase of TiO_2 . This material also differs substantially from other samples in terms of its electrochemical properties, which permits formulating the hypothesis that its variations in the phase composition and a higher concentration of nickel are responsible for the advantageous properties of the material.

Using sucrose instead of carbon soot in addition to the LTO resulted in high conductivity of the investigated materials. $\text{Li}_{3.8}\text{Cu}_{0.1}\text{Ni}_{0.1}\text{Ti}_5\text{O}_{12}\text{-C}$ and $\text{Li}_{3.8}\text{Cu}_{0.05}\text{Ni}_{0.15}\text{Ti}_5\text{O}_{12}\text{-C}$ have particularly high values of conductivity. Voltammograms of electrodes containing composite materials $\text{Li}_{3.8}\text{Cu}_{0.15}\text{Ni}_{0.05}\text{Ti}_5\text{O}_{12}\text{-C}$ and $\text{Li}_{3.8}\text{Cu}_{0.05}\text{Ni}_{0.15}\text{Ti}_5\text{O}_{12}\text{-C}$ have the correct course and are distinctive for LTO materials. The highest values were observed for the capacity of the relevant electrode $\text{Li}_{3.8}\text{Cu}_{0.05}\text{Ni}_{0.15}\text{Ti}_5\text{O}_{12}\text{-C}$.

For all materials, the obtained dependence of the capacity of the working electrode of the potential relative to a lithium electrode is typical for LTO materials. Three materials with stoichiometric composition $\text{Li}_{3.8}\text{Cu}_x\text{Ni}_{0.2-x}\text{Ti}_5\text{O}_{12}\text{-C}$ were obtained. Among the materials tested, the material $\text{Li}_{3.8}\text{Cu}_{0.05}\text{Ni}_{0.15}\text{Ti}_5\text{O}_{12}\text{-C}$ has by far the most advantageous properties (from the point of view of potential use in lithium-ion batteries). It is characterized by conductivity, the correct course of cyclic voltammetry and relatively high capacity (also for high discharge currents, higher than 1C).

From the point of view of safety and environmentally friendly production of Li-ion cells eliminating soot and applying $\text{Li}_{3.8}\text{Cu}_{0.05}\text{Ni}_{0.15}\text{Ti}_5\text{O}_{12}\text{-C}$ as an active material of an anode in lithium-ion batteries seems to be a good alternative to the currently used materials.

Acknowledgments

This work was supported by D. Olszewska's AGH University of Krakow subvention of the Ministry of Science and Higher Education in Poland.

REFERENCES

1. Wulandari T., Fawcett D., Majumder S.B., Poinern G.E.J. Lithium-based batteries, history, current status, challenges, and future perspectives. *Battery Energy* 2023; 2: e20230030, 1–53. <https://doi.org/10.1002/bte2.20230030>
2. Zhang H., Yang Y., Xu H., Wang L., Lu X., He X. $\text{Li}_4\text{Ti}_5\text{O}_{12}$ spinel anode: fundamentals and advances in rechargeable batteries. *InfoMat*. 2021; 4: e12228, 1–29. <https://doi.org/10.1002/inf2.12228>
3. Carella C. Global lithium-ion market to double despite recent issues in Report Frost & Sullivan; Mountain View, California, USA; 2013.
4. Cheng X.-B., Zhang R., Zhao C.-Z., Zhang Q. Toward safe lithium metal anode in rechargeable batteries: a review. *Chem. Rev.* 2017; 117: 10403–10473. <https://doi.org/10.1021/acs.chemrev.7b00115>
5. Künne S., Hesper J.M., Lein T., Voigt K., Mikhailova D., Michaelis A., Winter M., Placke T., Heubner Ch. Hybrid high-voltage $\text{LiNi}_{0.5}\text{Mn}_{1.5}\text{O}_4$ /graphite cathodes enabling rechargeable batteries with simultaneous an ion and cation storage. *Batteries & Supercaps* 2023; 6: e202300284, 1–12. <https://doi.org/10.1002/batt.202300284>
6. Zhang M., Zhong J., Kong W., Wang L., Wang T., Fei H., Luo H., Zhu J., Lu B. A high capacity and working voltage potassium-based dual ion batteries. *Energy Environ. Mater.* 2021; 4: 413–420 <https://doi.org/10.1002/eem2.12086>
7. Linden D., Reddy T.B. Handbook of Batteries (3rd Edition) McGraw-Hill, 2002.
8. Dong L., Wang Z., Li Y., Jin C., Dong F., Zhao W., Qin C., Wang Z. Spinel-structured, multi-component transition metal oxide $(\text{Ni}, \text{Co}, \text{Mn})\text{Fe}_2\text{O}_{4-x}$ as long-life lithium-ion battery anode material. *Batteries* 2023; 9: 54. <https://doi.org/10.3390/batteries9010054>
9. Li X., Zhu L., Yang C., Wang Y., Gu S., Zhou G. Core-shell structure trimetallic sulfide doped carbon composites as anodes for enhanced lithium-ion storage performance. *Molecules* 2023; 28: 7580. <https://doi.org/10.3390/molecules28227580>
10. Breczko J., Wysocka-Żołopa M., Grądzka E., Winkler K. Zero-dimensional carbon nanomaterials for electrochemical energy storage. *ChemElectroChem*. 2024; e202300752, 1–41. <https://doi.org/10.1002/celc.202300752>

11. Jia W., Zhang J., Zheng, L.; Zhou, H.; Zou, W.; Wang, L. Lithium-rich alloy as stable lithium metal composite anode for lithium batteries. *eScience*, 2024; <https://doi.org/10.1016/j.esci.2024.100266>.
12. Lou S., Zhano Y., Wang J., Yin G., Du Ch., Sun X. Ti-based oxide anode materials for advanced electrochemical energy storage: lithium/sodium ion batteries and hybrid pseudocapacitors. *Small* 2019; 15(52): 1904740. <https://doi.org/10.1002/sml.201904740>
13. Han X., Meng Q., Wan, X.S., Zhang Y., Shen B., Gao J., Ma Y., Zuo, P; Lou, S., Yin, G. Intercalation pseudocapacitive electrochemistry of Nb-based oxides for fast charging of lithium-ion batteries. *Nano Energy* 2021; 81: 105635. <https://doi.org/10.1016/j.nanoen.2020.105635>
14. Carbon-black. Available online: ICBA (carbon-black.org) (Accessed: 6 December 2024).
15. Zhu G., Du Y., Wang Y., Yu A., Xia Y., Electrochemical profile of lithium titanate/hard carbon composite as anode material for Li-ion batteries. *J. Electroanalytical Chem.* 2013; 688: 86–92. <https://doi.org/10.1016/j.jelechem.2012.07.035>
16. Gędziorowski B., Kondracki Ł., Świerczek K., Molenda J., Structural and transport properties of $\text{Li}_{1+x}\text{V}_{1-x}\text{O}_2$ anode materials for Li-ion batteries. *Solid State Ionics* 2014; 262: 124–127. <https://doi.org/10.1016/j.ssi.2013.12.001>
17. Odziomek M., Chaput F., Rutkowska A., Świerczek K., Olszewska D., Sitarz M., Lerouge F., Parola S. Hierarchically structured lithium titanate for ultrafast charging in long-life high capacity batteries. *Nature Communications* 2017; 8: 15636. <https://doi.org/10.1038/ncomms15636>
18. Wang J., Zhao H., Yang Q., Zhang T., Wang J. Electrochemical characteristics of $\text{Li}_{4-x}\text{Cu}_x\text{Ti}_5\text{O}_{12}$ used as anode material for lithium-ion batteries. *Ionics* 2013; 19: 415–419. <https://doi.org/10.1007/s11581-012-0771-3>
19. He Z., Wang Z., Wu F., Guo H., Li X., Xiong X. Spherical $\text{Li}_4\text{Ti}_5\text{O}_{12}$ synthesized by spray drying from a different kind of solution. *J. Alloys and Compounds* 2012; 540: 39–45. <https://doi.org/10.1016/j.jallcom.2012.06.044>
20. Li X.P., Mao J. A $\text{Li}_4\text{Ti}_5\text{O}_{12}$ -rutile TiO_2 nanocomposite with an excellent high rate cycling stability for lithium ion batteries. *New J. Chem.* 2015; 39: 4430–4436. <https://doi.org/10.1039/C5NJ00306G>
21. Olszewska D., Rutkowska A. Influence of the conditions of a solid-state synthesis anode material $\text{Li}_4\text{Ti}_5\text{O}_{12}$ on its electrochemical properties of lithium cells. *Bull. Mater. Sci.* 2018; 41: 16–25. <https://doi.org/10.1007/s12034-017-1540-8>
22. Chmielarz L., Dziembaj R., Grzybek T., Klinik J., Łojewski T., Olszewska D., Papp H. Pillared smectite modified with carbon and manganese as catalyst for SCR of NO_x with NH_3 . Pt. 1, General characterization and catalyst screening. *Catal. Lett.* 2000; 68: 95–100. <https://doi.org/10.1023/A:1019094327927>
23. Chmielarz L., Dziembaj R., Grzybek T., Klinik J., Łojewski T., Olszewska D., Węgrzyn A. Pillared smectite modified with carbon and manganese as catalyst for SCR of NO_x with NH_3 . Pt. 2. Temperature-programmed studies. *Catal. Lett.* 2000; 70: 51–56. <https://doi.org/10.1023/A:1019075502370>
24. Olszewska D. Ammonia and water sorption properties of the mineral-layered nanomaterials used as the catalysts for NO_x removal from exhaust gases. *Catal. Today* 2006; 114: 326–332.
25. Olszewska D. Application of modified montmorillonite for desulfurization during the combustion of hard coal. *Fuel Proc. Technol.* 2011; 92: 2412–2419.
26. Olszewska D. Application of XPS method in the research into Ni ion-modified montmorillonite as a SO_2 sorbent. *Fuel Proc. Technol.* 2012; 95: 90–95.
27. Sun X., Radovanovic P.V., Cui B. Advances in spinel $\text{Li}_4\text{Ti}_5\text{O}_{12}$ anode materials for lithium-ion batteries. *New J. Chem.* 2015; 39: 38–63. <https://doi.org/10.1039/C4NJ01390E>
28. Ouyang C., Zhong Z., Lei M. Ab initio studies of structural and electronic properties of $\text{Li}_4\text{Ti}_5\text{O}_{12}$ spinel. *Electrochem. Commun.* 2007; 9: 1107–1112. <https://doi.org/10.1016/j.elecom.2007.01.013>
29. Li B., Ning F., He Y., Du H., Yang Q., Ma J., Kang F., Hsu C. Synthesis and characterization of long life $\text{Li}_4\text{Ti}_5\text{O}_{12}/\text{C}$ composite using amorphous TiO_2 nanoparticles. *Int. J. Electrochem. Sci.* 2011; 6: 3210–3232. [https://doi.org/10.1016/S1452-3981\(23\)18246-0](https://doi.org/10.1016/S1452-3981(23)18246-0)
30. Ferg E., Gummow R.J., de Kock A. Spinel anodes for lithium-ion batteries. *J. Electrochem. Soc.* 1994; 141: 10–13. <https://doi.org/10.1149/1.2059324>
31. Choi M.-J., Baek J.H., Kim J.Y., Jang H.W. Highly textured and crystalline materials for rechargeable Li-ion batteries. *Battery Energy* 2023; 2: e20230010, 1–26 <https://doi.org/10.1002/bte.20230010>
32. Srout M., Carboni M., Gonzalez J.-A., Trabesinger S. Insights into the importance of native passivation layer and interface reactivity of metallic lithium lithium by electrochemical impedance spectroscopy. *Small* 2023; 19: e2206252, 1–10. <https://doi.org/10.1002/sml.202206252>
33. Lin C., Ding B., Xin Y., Cheng F., Lai M.O., Lu L.; Zhou H. J. Advanced electrochemical performance of $\text{Li}_4\text{Ti}_5\text{O}_{12}$ -based materials for lithium-ion battery: Synergistic effect of doping and compositing. *Power Sources* 2014; 248: 1034–1041. <https://doi.org/10.1016/j.jpowsour.2013.09.120>
34. Wang J.J., Zhao H., Yang Q., Zhang T., Wang J.J. Electrochemical characteristics of $\text{Li}_{4-x}\text{Cu}_x\text{Ti}_5\text{O}_{12}$ used as anode material for lithium-ion batteries. *Ionics*, 2013; 19: 415–419. <https://doi.org/10.1007/s11581-012-0771-3>

- org/10.1007/s11581-012-0771-3
35. Bai X., Li T., Wei C., Sun Y.-K., Qi Y.-X., Zhu H.-L., Lun N., Bai Y.-J. Enhancing the long-term cyclability and rate capability of $\text{Li}_4\text{Ti}_5\text{O}_{12}$ by simple copper-modification. *Electrochim. Acta* 2015; 155: 132–139. <https://doi.org/10.1016/j.electacta.2014.12.121>
 36. Scarpioni F., Khalid S., Chukwu R., Pianta N., Mantia F., Ruffo R. Electrochemical impedance spectroscopy for electrode process evaluation: lithium titanium phosphate in concentrated aqueous electrolyte. *ChemElectroChem* 2023; 10: e202201133, 1–12. <https://doi.org/10.1002/celec.202201133>
 37. Wang B., Cao J., Liu Y., Zeng T., Li L. Improved capacity and rate capability of Fe_2O_3 modified $\text{Li}_4\text{Ti}_5\text{O}_{12}$ anode material. *J. Alloys Compounds* 2014; 587: 21–25. <https://doi.org/10.1016/j.jallcom.2013.10.167>
 38. Ohzuku T., Ueda A., Yamamoto N., Zero-strain insertion material of $\text{Li}[\text{Li}_{1/3}\text{Ti}_{5/3}]\text{O}_4$ for rechargeable lithium cells. *J. Electrochem. Soc.* 1995; 142: 1431–1435. <https://doi.org/10.1149/1.2048592>
 39. Dahn J.R., Sleigh A.K., Shi H., Way B.M., Weydanz W.J., Reimers J.N., Zong Q., von Sacken U. Carbons and graphites as substitutes for the lithium anode. In: *Lithium batteries - new materials. Developments and Perspectives*; Pistoia, G., Ed.; Elsevier Amsterdam, Holland, 1994; 1–97.
 40. Yang G., Su Z., Fang H., Yao Y., Li Y., Yang B., Ma W. Synthesis and performance of $\text{Li}_4\text{Ti}_5\text{O}_{12}/\text{C}$ with little inert carbon. *Electrochim. Acta* 2013; 93: 158–162.
 41. Cunha D.M., Hendriks T.A., Vasileiadis A., Vos Ch.M., Verhallen T., Singh D.P., Wagemaker M., Huijben M. Doubling reversible capacities in epitaxial $\text{Li}_4\text{Ti}_5\text{O}_{12}$ thin film anodes for microbatteries. *ACS Appl. Energy Mater.* 2019; 2(5): 3410–3418. <https://doi.org/10.1021/acsam.9b00217>